Journal of Hazardous Materials 176 (2010) 361–366

Contents lists available at ScienceDirect

Journal of Hazardous Materials

journal homepage: www.elsevier.com/locate/jhazmat

Research article

Mild ring-opening coupling of liquid-phase cyclohexane to diesel components using sulfated metal oxides

Wei Mao, Hongzhu Ma*, Bo Wang

Institute of Energy Chemistry, School of Chemistry and Materials Science, Shaanxi Normal University, Xi'an 710062, People's Republic of China

ARTICLE INFO

Article history:
Received 24 June 2009
Received in revised form 4 November 2009
Accepted 4 November 2009
Available online 11 November 2009

Keywords:
Cyclohexane
Sulfated metal oxides
Liquid-phase
Diesel fuel

ABSTRACT

We have investigated a mild simple synthesis method for ring-opening coupling of liquid-phase cyclohexane to diesel components using various sulfated metal oxides [SO_4^{2-}/Fe_2O_3 (SF), SO_4^{2-}/TiO_2 (ST) and SO_4^{2-}/ZrO_2 (SZ)] under low temperature (333 K) and atmospheric pressure. Neither solvent nor promoters are needed in the reaction system so as to be a clean approach. Operating under these reaction conditions, a maximum activity of 6% was obtained with SF as catalyst, and a significantly high selectivity of 74.5% for nicer diesel components (n-C_{14}–C_{18}) was obtained simultaneously. Whereas, ST and SZ displayed low activity for cyclohexane reaction. By utilization of the temperature-programmed desorption of ammonia (NH_3-TPD) measurement and the N_2 adsorption method, the results suggested that a satisfied acid strength distribution and high density of acid sites appeared in SF catalyst in comparison with other catalysts, which may play an important role in the reaction.

1. Introduction

In recent years, although global oil reserves have been increasingly dwindled, the petroleum-derived fuels still play an important role in human society. In particular, the diesel fuel is increasingly embraced in public transportation, power generation, large instrument, e.g. due to its excellent fuel efficiency [1–5]. Consequently, to meet above consumption as well as the shortage of petroleum resources, the expansion of diesel fuel production is to some extend considered as a reasonable and effective strategy for exploiting unsustained petroleum resources.

In general, the diesel fuel is a blend of liquid compounds derived from petroleum distillates, which is mainly made up of aliphatic hydrocarbons containing 10–24 carbon atoms with boiling points in the range of 150–400 °C [5]. Furthermore, diesel fuel is classified according to its ignition quality as measured by cetane number (CN), and linear paraffins have the highest cetane number, followed by linear olefins, branched paraffins, and cycloparaffins, and the lowest CN is obtained by aromatics [6]. On the other hand, cycloalkane is an important component in conventional fuel (up to 3% in gasoline and up to 35% in diesel fuel) [7], and many of reports have described the cycloparaffins such as cyclohexane and methylcyclopentane, ring opening and isomerization reaction so as to obtain high quality gasoline [8,9]. The main products for both reactants are C_6 branched isomers (n-hexane, 2-methylpentane, and 3-methylpentane). However, relatively little attention has been paid to the chemistry involved in their ring-opening coupling (ROC) reaction for producing high molecular weight alkanes in the diesel range, which is an attractive scheme for upgrading low-value cycloparaffins into the desired high-CN diesel component.

Up to now, numerous research has shown that the two reaction of ring opening and coupling can be carried out by strong solid acid catalysts [4,10–12]. Moreover, an appropriate distribution of acid sites for catalysts is needed in order to avoid secondary cracking that compete for the same active sites. Thus, in order to develop ROC reactions, a catalyst with both strong acid strength and well acid sites distribution is required. On the other hand, during the last decade, sulfated metal oxides have been one of the most studied solid acids owing to their strong acidity and high activity in various organic reactions such as ring opening, coupling and alkylation at mild temperatures [12–16]. Among various catalysts, sulfated zirconia, sulfated titania and sulfated iron oxide have attracted much attention due to their superacidity and high activity in low temperature, of which $H_0 < -16$, $H_0 < -14$ and $H_0 < -12$ (the Hammett function scale), in sequence [14–16].

Herein, we focus on the ROC of cyclohexane with SO_4^{2-}/Fe_2O_3 (SF), SO_4^{2-}/TiO_2 (ST) and SO_4^{2-}/ZrO_2 (SZ) as catalysts under mild conditions, and attempt to carry out the selective conversion of cyclohexane to alkanes in the diesel range. The purpose of our paper is to ascertain if above-mentioned sulfated oxides can act as effective catalysts for ROC of cyclohexane to diesel component under mild conditions. In addition, in order to compare the roles of various catalysts for cyclohexane conversion, various techniques such as X-ray diffraction (XRD), Fourier transform infrared spectroscopy (FT-IR) and energy dispersive X-ray spectroscopy (EDX) were employed to characterize catalysts.

* Corresponding author. Tel.: +86 29 85303324; fax: +86 29 85307774.
E-mail address: hzmachem@snnu.edu.cn (H. Ma).

0304-3894/$ – see front matter © 2009 Elsevier B.V. All rights reserved.
doi:10.1016/j.jhazmat.2009.11.036

2. Experimental

2.1. Catalyst preparation

All chemicals used in the experiment were analytically pure grade without any further purification. $ZrOCl_2{\cdot}8H_2O$, $Fe(NO_3)_3{\cdot}9H_2O$ and $TiC1_4$ were purchased from Shanghai Reagent Co., China, and polyethylene glycol, ethanol and cyclohexane were obtained from Xi'an Reagent Co.

Zirconium hydroxide samples were prepared by modified precipitation method as follow, and similar method has been reported by Martínez et al. [17]. An aqueous solution of zirconium oxychloride (1.34 M) and aqueous ammonia (25%) were added concurrently dropwise to a stirred aqueous polyethylene glycol up to pH 9 in ice-water bath. The obtained precipitates were aged at ambient temperature and atmospheric pressure for 24 h. Then, the precipitates were filtrated, washed with distilled water thoroughly until freed from chloride ions and dried at 373 K for 24 h. The precipitate of iron hydroxide was also obtained according to the procedures described above, using $Fe(NO_3)_3{\cdot}9H_2O$ (2.5 M) as a source of iron ions.

The H_4TiO_4 was prepared by hydrolyzing $TiC1_4$ as follows. In the first stage, a solution of titanium tetrachloride (30 mL) was added drop-by-drop to a stirred anhydrous ethanol up to the hydroxide sol obtained in ice-water bath. In the second stage, aqueous ammonia was added dropwise to above system until pH 8. Other procedures were carried through as above.

The sulfated metal oxides were obtained by sulfating the amorphous hydroxides with 1.0 M sulfuric acid solution (4 mL acid solution per 1 g sample) at room temperature for 2 h with agitation so as to obtain a 9 wt.% S, followed by solvent evaporation and drying (one step) and calcined in a muffle furnace at 500 °C for 3 h (ST, SF) and at 550 °C for 3 h (SZ).

2.2. Reaction procedure

In this paper, the ROC of cyclohexane over SZ, ST and SF under mild conditions was carried out under the following typical procedures. The reactant, cyclohexane (100 mL) and catalyst (5 g) were charged into a simple slurry reactor system (Pyrex glass, 150 mL) at 333 K and atmospheric pressure in the air, and the agitation rate during reaction was maintained at 150 rpm. Prior to the reaction, the catalyst was activated at 363 K for 1.0 h in dry air. The reaction mixtures were drawn out at regular intervals and analyzed by gas chromatography–mass spectrometry (GC–MS, QP2010, Japan, DB-5MS 30 m/0.25 mm/250 mm polyethyleneglycol column), and the peak of reactant was taken off in order to prevent overload of MS detector during GC–MS testing. Each catalyst test was performed for a period of at least 6 h. Analysis of numerous products obtained in this conversion is not straightforward, and many standard compounds were used to confirm the identity of the compounds. The conditions of chromatography: injection temperature, 280 °C; initial temperature, 50 °C for 2 min; ramp 1, 7.0 °C/min to 280 °C, held for 5 min. Moreover, the amount of reaction products was analyzed by the same GC with FID, using the iso-octane as an internal standard.

Conversion at reaction time t is calculated on the consumed cyclohexane (C_0 represents the initial concentration of cyclohexane, whereas C_t represents the concentration of cyclohexane at reaction time t):

$$\text{conversion}\,\% = \frac{C_0 - C_t}{C_0} \times 100\%$$

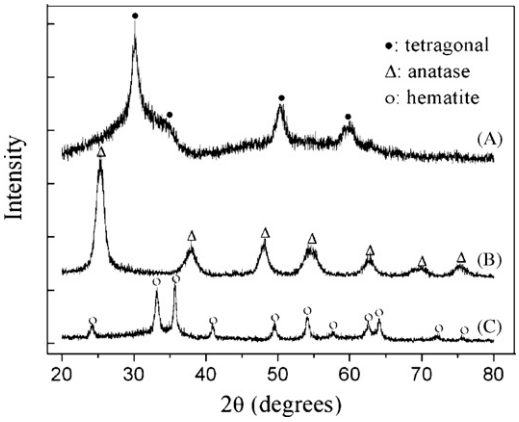

Fig. 1. X-ray diffraction patterns of sulfated metal oxides: (A) SZ calcined at 550 °C for 3 h, (B) ST and (C) SF calcined at 500 °C for 3 h.

2.3. Catalyst characterization

XRD analyses were performed to characterize the bulk properties of the catalysts. XRD patterns of the as-prepared samples were collected with a Rigaku D/max-γA rotation anode X-ray diffractometer (Cu Kα, λ = 0.15418 nm). The pattern for the structure refinement was taken in a 2θ range of 20–80° with a step width of 0.02° (2θ). The infrared absorptions were studied adopting FT-IR spectrometer (Nicolet Avatar360E) for investigating the nature of bonding of sulfate ion on the catalysts, and the IR spectra of catalyst was recorded at room temperature on a 5% sample of KBr disk. Before disks were made, all the samples were degassed at 383 K for 1 h in vacuum. The temperature-programmed desorption of ammonia (NH_3-TPD) measurement was carried on an AutoChem II 2920 instrument (Micromeritics, USA) for comparing the relative acid strengths and acidic sites of sulfated samples. Prior to TPD studies, a sample of 0.1 g was first pretreated in pure Ar at 773 K for 60 min, then cooled to 373 K and saturated at this temperature with anhydrous ammonia gas (10% in Ar) for 30 min. Weakly adsorbed NH_3 was eliminated by treatment under Ar at the same temperature for 60 min. The NH_3-TPD profile was recorded with a thermal conductivity detector with a heating rate of 10 K min^{-1} from 373 to 873 K in an Ar flow. The surface area of the catalysts was measured using nitrogen adsorption at 77 K and the Brunauer–Emmett–Teller (BET) method using a Micrometerics ASAP2020 system. The signals of surface elements were detected by EDX (Oxford Instruments Microanalysis 1350) mapping method.

3. Results and discussion

3.1. Characterization of sulfated metal oxides

The X-ray powder diffraction patterns of sulfated oxides samples (Fe, Ti, Zr) are shown in Fig. 1. Although it can been seen that the hematite phase of Fe_2O_3 (PDF-ICDD 89-2810), the anatase phase of TiO_2 (PDF-ICDD 89-4921) and the tetragonal phase of ZrO_2 (PDF-ICDD 88-1007) appear to XRD diffraction, all the samples exhibit weak intensity and broad diffraction patterns due to poor crystalline state and small particles possibly. Moreover, no diffraction peaks due to corresponding metal sulfate compounds appear. Several papers have reported that impregnated sulfate ions retard crystallization process from amorphous to crystalline and prevent crystallite agglomeration during calcination so that high surface area are obtained in samples [18–20], which is in line with the BET results.

The results of IR spectra of sulfated oxides are presented in Fig. 2. Four shoulder bands at 1207, 1125, 1039 and 985 cm^{-1} appear in

Table 1
Products distribution in ROC of cyclohexane over various catalysts.[a].

Catalyst	Products selectivity (%)[b]						Nicer diesel components yield (%)[c]
	n-C_{14}	n-C_{15}	n-C_{16}	n-C_{17}	n-C_{18}	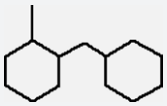	
SF	9.5	8.2	23.4	6.2	27.2	18.6	4.47
ST	6	4.3	11.4	8.4	14.8	41.6	1.8
SZ					[d]		

[a] Reaction conditions: reaction temperature 333 K and atmospheric pressure, 360 min.
[b] The selectivity is based on mol%.
[c] Nicer diesel components are the sum of n-C_{14}–C_{18}.
[d] Too low amounts for a reliable value.

the curve of SF sample calcined at 500 °C, correspond to the characteristic frequencies of bidentate sulfate ion coordinated to the metal such as Zr, Ti [16,21–23]. The similar absorption bands at 1213, 1131 and 1039 cm^{-1} are also possessed by the ST sample. However, only a broad band at 1128–1042 cm^{-1} appear in the curve of SZ, which can be due to the overlapping of the ZrO_2 skeletal vibration [23]. In general, for the metal oxides modified with sulfate ions followed by evacuation above 400 °C, a strong band assigned to S=O asymmetric stretching frequency of SO_4^{2-} can be observed at 1300–1400 cm^{-1} [16,23], which is believed to be a driving force in the generation of superacidic property on sulfated metal oxides. Herein, except the band at 1391 cm^{-1} in the ST sample can be observed, the corresponding bands can be hardly seen in other samples, which may be due to the absorded H_2O molecules on the surface of samples. Similar findings were reported by Babou et al. and Sohn et al. [22,23].

3.2. Catalytic properties

The conversion of cyclohexane was determined over various catalysts at 333 K and atmospheric pressure; the activities of sulfated metal oxides catalysts are shown in Fig. 3 as a function of reaction time. It shows that although the catalysts of SF and ST display similar trend in catalytic activities both initial activities and steady activities, SZ shows a significantly lower activity in comparison with above two catalysts. The activity after 360 min was found to be different for all samples, and a maximum conversion of 6% was obtained on SF, whereas SZ gave a lowest conversion of 0.9% in the same conditions. From these results it is readily apparent that the SF is more active than other catalyst at these conditions. Furthermore, the cyclohexane conversion did not increase steadily with the reaction time prolongation in ST and SF, and a dramatically increase of conversion can be observed after 240 min in above systems that could not be observed for SZ, indicating an induction period for ROC of cyclohexane may appear at the beginning of the reaction. It is consistent with the reported fact that an slow induction period can be observed in catalytic performance of sulfated metal oxides with alkanes under low temperature [24–26], which involve a redox mechanism that result in a formation of olefins on the catalyst surface. On the other hand, the results for products distribution obtained in various catalysts are presented in Table 1, where data are taken at reaction time of 360 min. The major products of ROC of cyclohexane are tetradecane, pentadecane, hexadecane, heptadecane, octadecane and 1-(cyclohexylmethyl)-2-methylcyclohexane with only trace amounts of 3,7-dimethylnonane, 2,6,10-trimethyldodecane and 1-tert-butyl-4-methylcyclohexane, indicating desired diesel components are synthesized over prepared catalysts under mild conditions, and other products are not observed in the case of these catalysts after 360 min. Moreover, SF exhibits a similar products distribution to ST but the highest diesel component yield (5.6%) among all catalysts tested in this investigation so that SF is the best catalyst in our work in terms of diesel component production (the GC–MS results of SF is shown in Fig. 4).

On the other hand, the strong adsorption phenomena of reaction molecules may occur on catalyst surface, which were hardly desorbed at low temperature in our investigation. This result was coincident with EDX analysis, where the concentration of carbon element reached to 35.6 mol% on used SF catalyst that was not detected in fresh catalyst. Additionally, this result also indicated the conversion values at the initial stages may be false by the carbon balance disturbance, similar discussion has been reported by Lutecki and Breitkopf [26]. Moreover, the observed carbon on used catalyst may also indicated that deactivation occurred during

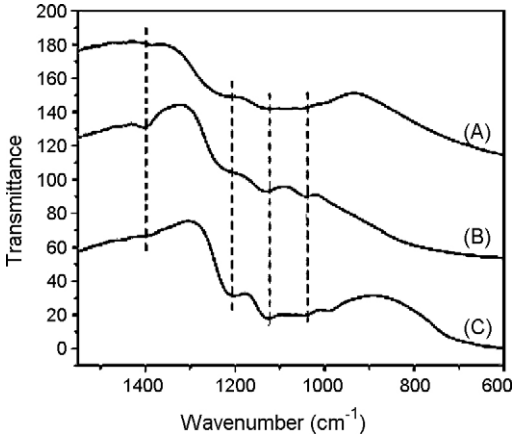

Fig. 2. FT-IR spectra of various catalysts: (A) SO_4^{2-}/ZrO_2 (SZ), (B) SO_4^{2-}/TiO_2 (ST) and (C) SO_4^{2-}/Fe_2O_3 (SF).

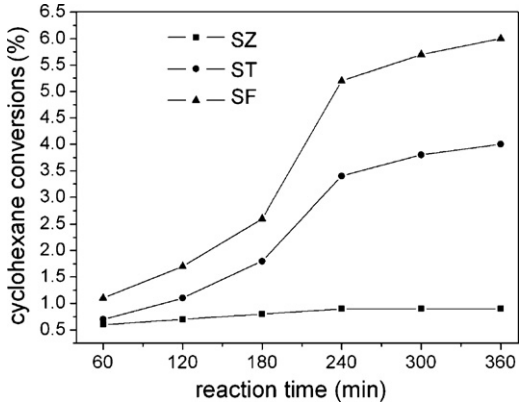

Fig. 3. Conversions of cyclohexane over various catalysts in function of reaction time. Solid square, SZ; solid circle, ST; solid triangle, SF.

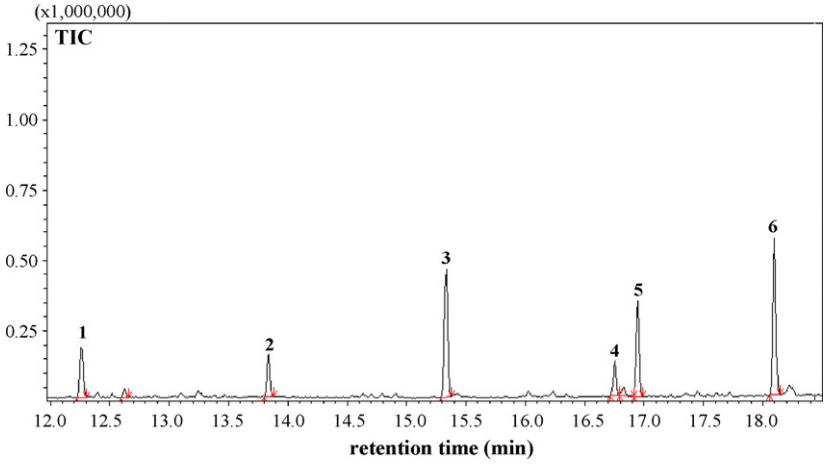

Fig. 4. The total ion chromatogram of the products for SF (360 min), and corresponding MS Date. *m*/*e* (relative intensity): (1) Tetradecane, 40(0.7), 41(43.5), 42(13), 43(80.2), 44(2), 53(0.8), 55(21.5), 56(19.8), 57(100), 58(3.6), 67(2.7), 69(7.2), 70(12.7), 71(66.3), 72(2.2), 82(0.8), 83(9), 84(8.2), 85(39.4), 86(0.8), 97(4.4), 98(4.1), 99(8.8), 112(3.2), 113(4), 126(1.8), 127(1.00), 140(0.8), 141(0.8), 198(1). (2) Pentadecane, 41(38.6), 42(13.5), 43(72.1), 55(16.2), 56(24.1), 57(100), 58(5.2), 66(5.5), 69(6.2), 70(14), 71(52.6), 72(2.5), 81(3.2), 83(11.7), 84(8.8), 85(50.6), 95(2.1), 97(9.8), 98(3), 99(10.6), 111(1), 112(2.5), 113(6), 126(2.1), 127(2.2), 212(1). (3) Hexadecane, 40(3.8), 41(32.4), 42(8.1), 43(66.3), 44(3.7), 53(1), 54(1.4), 55(17.9), 56(16), 57(100), 58(3.8), 66(3.1), 68(1.1), 69(15.4), 70(10), 71(53.1), 72(2.5), 81(1.3), 82(1.8), 83(8.6), 84(5.7), 85(36.2), 86(1.9), 95(0.3), 96(0.3), 97(6.3), 98(3.9), 99(9.6), 100(0.6), 111(1.7), 112(2.6), 113(5), 126(2.4), 127(3.6), 140(1.8), 141(1.8), 154(0.8), 155(1.5), 169(0.7), 226(2). (4) Heptadecane, 39(4.6), 41(40.1), 42(12.8), 43(70.9), 44(3.3), 55(14.3), 56(23.3), 57(100), 58(5), 69(6.5), 70(15.4), 71(2), 72(1.8), 81(2.8), 82(1.4), 83(14.4), 84(9), 85(39), 98(3.2), 99(16.1), 111(4.5), 112(1.4), 113(7.6), 127(3.5), 141(1.5). (5) 1-(Cyclohexylmethyl)-2-methylcyclohexane, 41(21.3), 42(1.9), 43(22.4), 53(3.8), 55(19.3), 56(1.1), 57(57.5), 58(3.3), 67(9.3), 68(0.6), 69(14), 70(3), 77(2.1), 79(6.5), 81(17.9), 82(12.6), 83(13.6), 84(6.2), 91(3.3), 93(3.2), 95(9.9), 96(8.7), 97(100), 98(12.2), 99(22), 100(1.2), 105(0.5), 107(3.1), 109(9.9), 110(2.7), 111(11.4), 112(1.9), 123(18.6), 124(5.1), 125(5.2), 137(11.6), 138(5.9), 139(0.5), 151(4.2), 165(3), 179(8.4), 180(6.9), 193(0.5), 292(1.3). (6) Octadecane, 40(0.3), 41(31.9), 42(10.5), 43(71.2), 44(4.4), 53(1), 54(1.8), 55(18.4), 56(11.2), 57(100), 58(4.6), 67(4.6), 68(1.8), 69(11.7), 70(12.9), 71(67.7), 72(3.5), 82(2.6), 83(3.1), 84(6.9), 85(39.1), 86(2.5), 96(1.3), 97(12.1), 98(4), 99(14.2), 100(0.6), 109(0.3), 110(0.3), 111(3.4), 112(3.1), 113(8.9), 125(1), 126(2.4), 127(5.3), 140(1.9), 141(3.1), 154(1.4), 155(2.1), 168(0.6), 169(1.6), 183(1), 197(0.6), 254(2.3).

catalytic cycle so that a low conversion was obtained throughout reaction process, and above phenomena was also discussed by Lutecki and Breitkopf [26]. According to the unusual product distribution in this case, it implied the reaction path on prepared catalyst did not proceed via the typical monomolecular or the bimolecular mechanism which play an important role in catalytic performance of sulfated metal oxides. It may be conceivable that small molecules as the intermediate species from cyclohexane ring opening on catalyst by the redox mechanism may undergo similar oligomerization or coupling on other active sites, resulting in long chain hydrocarbon. Analogous reactions over SO_4^{2-}/M_xO_y have been reported in the literatures [12,27]. In view of this point, the acidity of catalyst may be an indication towards the explanation of complicated interplay of reaction path and active centres on catalyst, although the observation of possible intermediates is very difficult at this moment for the special catalytic behavior which will be investigated further.

The acidity is one of the important properties required from sulfated oxides used as catalysts, which plays a major role in the process of ring opening and coupling reaction, and the NH_3-TPD is a simple method widely used for investigating both the strength and number of acid sites present on the surface of an acidic solid. Furthermore, it should be pointed out that although partial sulfate groups may decompose at high temperature during TPD testing, ammonia is an acceptable probe molecule for qualitative analysis of the acidic properties of solid catalysts in our experimental conditions, which is consistent with previous works [28,29]. Different NH_3-TPD profiles are obtained for all sulfated oxides in Fig. 5 and the corresponding total acidity results based on the integrated area under the TPD curve to the mass amount of desorbed NH_3 are presented in Table 2. It can be observed markedly that a broad NH_3 desorption profile in the range 100–470 °C with two desorption maximum around 185 and 370 °C, respectively, appears in the case of SF sample, corresponding to ammonia chemisorbed on weak and medium acid sites, respectively [13,16]. Additionally, a high temperature desorption peak about 490–590 °C also appears in the curve of SF, indicating the formation of superacid sites [13,16], although the high temperature peak may also contain the partial decomposition of the sulfate ions. Whereas, the desorption patterns of SZ show different shapes to that of SF, only a broad peak with maximum intensity about 250 °C and a high temperature desorption peak between 515 and 570 °C appear. Furthermore, a different high temperature desorption peak with two desorption maximum around 450 and 510 °C is present in the curve of ST sample. By comparing various TPD-profiles, it is seen that although all samples have both weak and superacid acid sites, only SF has a notable high concentration of acid sites with the medium strength, indicating a more broad acid strength distribution is presented in SF. Thus, in view of various catalysts activities, it may be reasonable to infer that broad acid strength distribution for SF account for its high activity in the ROC of cyclohexane under mild conditions.

On the other hand, all samples display approximate total integrated area corresponds to the mass amount of desorbed NH_3, which are proportional to total acidities of samples. Moreover, considering different BET areas of catalysts, it is readily appar-

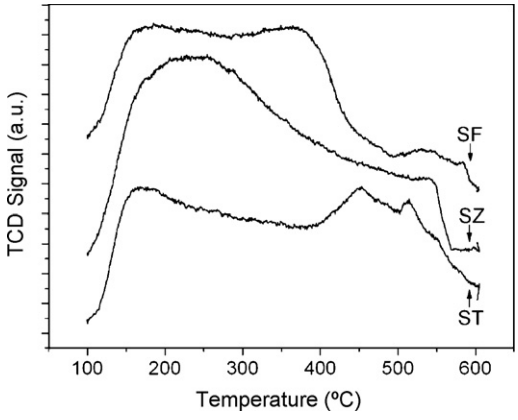

Fig. 5. The profiles for temperature-programmed desorption of ammonia on various sulfated oxides.

Table 2
Physico-chemical characterization and acid properties of prepared samples.

Samples	S_{BET} ($m^2\ g^{-1}$)[a]	D_{BJH} (nm)[b]	Crystallite size (nm)[c]	S/M (mole rate)[d]	Integrated area[e]
SF	55	6.23	0.253	0.12	2256.4
ST	103	2.68	0.351	0.13	2258.9
SZ	115	2.33	0.295	0.17	2259.2

[a] BET surface area calculated from the linear part of the BET plot ($P/P_0 = 0.2$).
[b] Average pore diameter, estimated using the desorption branch of the isotherm and the Barrett–Joyner–Halenda (BJH) formula.
[c] Average crystal size of hematite–Fe_2O_3, anatase–TiO_2 or tetragonal–ZrO_2, estimated using Scherrer equation.
[d] The mole rate of S to metal element on the surface of various samples determined by EDX.
[e] Integrated area under the TPD curve corresponds to the mass amount of desorbed NH_3.

ent that a maximum total number of acid sites per unit area is obtained in SF. In combination with the results of reaction products, it may be reasonable to infer that high density of acid sites and large pore diameter can promote the catalytic reaction of cyclohexane towards diesel components, which raise the possibility of interaction between intermediates from ring opening, leading to formation of long chain hydrocarbon. It should be noted that the presumed ring opening, oligomerization and coupling reaction in this catalytic cycle involve complicated interplay of reactant on various active sites of catalyst surface, including Lewis and Brønsted sites, which has been reported in the literature [27,30,31]. Besides, since all the samples are not remarkably active, it seems that external surface and big porous region are mainly responsible for the catalytic sites, whereas internal areas derived from small pore are inactive in the reaction. Perhaps, the high reactivity of SF is related to its largest external surface in comparison with other catalysts. Thus, although SZ has strong acid strength and largest BET area, it is inactive in ROC of cyclohexane. The point to emphasize here is that the adsorbed carbon on surface active sites may also restrict the increasing of conversion, leading to catalyst deactivation. In this regard, the used catalyst was regenerated by calcination at 623 K for 3 h, which was then employed at the same reaction conditions twice. The conversion was almost unchanged during two runs, indicating the regenerated catalyst has almost the same activity as the fresh catalyst. In addition, it is interesting to compare this investigation with our previous work [32], although SF display less cyclohexane conversion than V-promoted sulfated ZrO_2, it is more environmentally benign and low-cost, and our work also confirms that diesel components can be produced without air flow.

4. Conclusion

Overall, we have demonstrated the potential of ROC process for making high molecular weight alkanes in the diesel range one-step from liquid-phase cyclohexane over SO_4^{2-}/M_xO_y (M = Zr, Ti, Fe) under mild conditions. Moreover, it is interesting to find that SO_4^{2-}/Fe_2O_3 is capable of catalyzing the ROC of cyclohexane into diesel components with highest activity in comparison with other catalysts. In addition, this process is environmentally benign as it occurs at low temperature (333 K) and atmospheric pressure and solid acids eliminate the toxic and corrosive properties. However, one of the shortcomings for this catalyzed process with SO_4^{2-}/Fe_2O_3 is that the conversion is not high, future work on the ROC of cyclohexane requires to find well support to load above catalyst in order to increase the conversion. In summary, this work represents a new advance in the greening of ring-opening coupling process used to transfer cyclohexane to nicer diesel components.

Acknowledgment

We are grateful to be supported in part by the Innovation Funds of Graduate Programs, Shaanxi Normal University (No. 2009CXS011).

References

[1] B.H. Cooper, B.B.L. Donnis, Aromatic saturation of distillates: an overview, Appl. Catal. A 137 (1996) 203–223.
[2] A.P. Walker, Controlling particulate emissions from diesel vehicles, Top. Catal. 28 (2004) 1–4.
[3] E.W.D. Menezes, R.D. Silva, R. Cataluña, R.J.C. Orteg, Effect of ethers and ether/ethanol additives on the physicochemical properties of diesel fuel and on engine tests, Fuel 85 (2006) 815–822.
[4] H.B. Du, C. Fairbridge, H. Yang, Z. Ring, The chemistry of selective ring-opening catalysts, Appl. Catal. A 294 (2005) 1–21.
[5] B.D. Batts, A.Z. Fathoni, A literature review on fuel stability studies with particular emphasis on diesel oil, Energy Fuels 5 (1991) 2–21.
[6] F. Locatelli, J.P. Candy, B. Didillon, G.P. Niccolai, D. Uzio, J.M. Basset, Hydrogenolysis of cyclohexane over Ir/SiO_2 catalyst: a mechanistic study of carbon–carbon bond cleavage on metallic surfaces, J. Am. Chem. Soc. 123 (2001) 1658–1663.
[7] F. Buda, B. Heyberger, R. Fournet, P.A. Glaude, V. Warth, F.B. Leclerc, Modeling of the gas-phase oxidation of cyclohexane, Energy Fuels 20 (2006) 1450–1459.
[8] C. Jiménez, F.J. Romero, R. Roldán, J.M. Marinas, J.P. Gómez, Hydroisomerization of a hydrocarbon feed containing n-hexane, n-heptane and cyclohexane on zeolite-supported platinum catalysts, Appl. Catal. A 249 (2003) 175–185.
[9] G.R. Gattorno, L.O. Alemán-Vázquez, X. Angeles-Franco, J.L. Cano-Domínguez, R. Villagómez-Ibarra, Cyclohexane ring opening on alumina-supported Rh and Ir nanoparticles, Energy Fuels 21 (2007) 1122–1126.
[10] M. Santikunaporn, J.E. Herrera, S. Jongpatiwut, D.E. Resasco, W.E. Alvarez, E.L. Sughrue, Ring opening of decalin and tetralin on HY and Pt/HY zeolite catalysts, J. Catal. 228 (2004) 100–113.
[11] G.B. McVicker, M. Daage, M.S. Touvelle, C.W. Hudson, D.P. Klein, W.C. Baird, B.R. Cook, J.G. Chen, S. Hantzer, D.E.W. Vaughan, E.S. Ellis, O.C. Feeley, Selective ring opening of naphthenic molecules, J. Catal. 210 (2002) 137–148.
[12] M. Hinoa, K. Arata, Conversion of propane into butanes catalyzed by sulfated zirconia mixed with Pt/ZrO_2, Chem. Commun. (1999) 53–54.
[13] B.M. Reddya, P.M. Sreekanth, Y. Yamada, Q. Xu, T. Kobayashi, Surface characterization of sulfate, molybdate, and tungstate promoted TiO_2-ZrO_2 solid acid catalysts by XPS and other techniques, Appl. Catal. A 228 (2002) 269–278.
[14] K. Satoh, H. Matsuhashi, K. Arata, Alkylation to form trimethylpentanes from isobutane and 1-butene catalyzed by solid superacids of sulfated metal oxides, Appl. Catal. A 189 (1999) 35–43.
[15] S. Furuta, H. Matsuhashi, K. Arata, Catalytic action of sulfated tin oxide for etherification and esterification in comparison with sulfated zirconia, Appl. Catal. A 269 (2004) 187–191.
[16] T. López, P. Bosch, F. Tzompantzi, R. Gómeza, J. Navarrete, E. López-Salinas, M.E. Llanos, Effect of sulfation methods on TiO_2–SiO_2 sol–gel catalyst acidity, Appl. Catal. A 197 (2000) 107–117.
[17] A. Martínez, G. Prieto, M.A. Arribas, P. Concepción, J.F. Sánchez-Royo, Influence of the preparative route on the properties of WO_x–ZrO_2 catalysts: a detailed structural, spectroscopic, and catalytic study, J. Catal. 248 (2007) 288–302.
[18] K.M. Parida, N. Sahu, N.R. Biswal, B. Naik, A.C. Pradhan, Preparation, characterization, and photocatalytic activity of sulfate-modified titania for degradation of methyl orange under visible light, J. Colloid Interface Sci. 10 (2007) 28–34.
[19] S.B. Wang, K. Murata, T. Hayakawa, S. Hamakawa, K. Suzuki, Oxidative dehydrogenation of ethane over alkali metal doped sulfated zirconia catalysts, J. Chem. Technol. Biotechnol. 74 (1999) 988–992.
[20] A. Patel, G. Coudurier, N. Essayem, J.C. Védrine, Effect of the addition of Sn to zirconia on the acidic properties of the sulfated mixed oxide, J. Chem. Soc. Faraday Trans. 93 (1997) 347–353.
[21] J.R. Sohn, S.H. Lee, J.S. Lim, New solid superacid catalyst prepared by doping ZrO_2 with Ce and modifying with sulfate and its catalytic activity for acid catalysis, Catal. Today 116 (2006) 143–150.
[22] F. Babou, G. Coudurier, J.C. Vedrine, Acidic properties of sulfated zirconia: an infrared spectroscopic study, J. Catal. 152 (1995) 341–349.
[23] J.R. Sohn, J.G. Kim, T.D. Kwon, E.H. Park, Characterization of titanium sulfate supported on zirconia and activity for acid catalysis, Langmuir 18 (2002) 1666–1673.
[24] D.S. Satoh, H. Matsuhashi, H. Nakamura, K. Arata, Isomerization of cycloheptane, cyclooctane, and cyclodecane catalyzed by sulfated zirconia—comparison with open-chain alkanes, Phys. Chem. Chem. Phys. 5 (2003) 4343–4349.
[25] X.B. Li, K. Nagaoka, L.J. Simon, R. Olindo, J.A. Lercher, A. Hofmann, J. Sauer, Oxidative activation of n-butane on sulfated zirconia, J. Am. Chem. Soc. 127 (2005) 16159–16166.

[26] M. Lutecki, C. Breitkopf, Improvement of the catalytic isomerization performance for sulfated zirconias by use of templating techniques, Appl. Catal. A 352 (2009) 171–178.
[27] A. Mantilla, F. Tzompantzi, G. Ferrat, A. López-Ortega, E. Romero, E. Ortiz-Islas, R. Gómez, M. Torres, Room temperature olefins oligomerization over sulfated titania, Chem. Commun. (2004) 1498–1499.
[28] F. Lónyi, J. Valyon, J. Engelhardt, F. Mizukami, Characterization and catalytic properties of sulfated ZrO_2–TiO_2 mixed oxides, J. Catal. 160 (1996) 279–289.
[29] A.L.C. Pereira, S.G. Marchetti, A. Albornoz, P. Reyes, M. Oportus, M.D.C. Rangel, Effect of iron on the properties of sulfated zirconia, Appl. Catal. A 334 (2008) 187–198.
[30] M. Pérez, H. Armendáriz, J.A. Toledo, A. Vázquez, J. Navarrete, A. Montoya, A. Gárcia, Preparation of Ni/ZrO_2-SO_4^{2-} catalysts by incipient wetness method: effect of nickel on the isomerization of *n*-butane, J. Mol. Catal. A 149 (1999) 169–178.
[31] R.L. Martins, M. Schmal, Methane activation on superacidic catalysts based on oxoanion modified zirconium oxide, Appl. Catal. A 308 (2006) 143–152.
[32] B. Wang, J.J. Wang, H.Z. Ma, Synthesis of linear alkane (C_{14}–C_{28}) from cyclohexane with V-promoted sulfated ZrO_2 under mild conditions, Energy Fuels 22 (2008) 218–222.